Impact of Approximating the Initial Bubble Pressure on Cell Nucleation in Polymeric Foaming Processes

Siu N. Leung, Hongbo Li, Chul B. Park

Microcellular Plastics Manufacturing Laboratory, Department of Mechanical & Industrial Engineering, University of Toronto, Toronto, Ontario, Canada M5S 3G8

Received 31 March 2006; accepted 3 November 2006
DOI 10.1002/app.25728
Published online in Wiley InterScience (www.interscience.wiley.com).

ABSTRACT: According to the classical nucleation theory, the free energy barrier for bubble nucleation, and thereby the nucleation rate, are functions of the initial bubble pressure, $P_{bubble,0}$. In almost all of the previous studies that have used computer simulations to investigate polymeric foaming processes, the value of $P_{bubble,0}$ has been approximated using the saturation pressure, P_{sat}. This article employs the thermodynamic equilibrium condition and the Sanchez–Lacombe (SL) equation of state (EOS) to determine the value of $P_{bubble,0}$. It is shown that using P_{sat} to approximate $P_{bubble,0}$ may lead to significant overestimations of the nucleation rate and the final cell density. © 2007 Wiley Periodicals, Inc. J Appl Polym Sci 104: 902–908, 2007

Key words: bubble pressure approximation; computer simulation; nucleation; polymeric foaming process

INTRODUCTION

Polymeric foaming is a complex process that involves delicate thermodynamic phenomena and kinetic material transport. It is very challenging to completely control all aspects of the cell morphologies in various polymeric foaming technologies. Since cell nucleation and growth are the factors that predominantly govern the final foam structures and quality, a fundamental understanding of the underlying mechanisms of these processes is indispensable to improve their regulation and to optimize different processing technologies utilized in the foaming industry.

In this context, researchers have attempted to investigate the foaming processes from both experimental and theoretical perspectives. Extensive experimental studies have focused on exploring the effects of various processing parameters (i.e., temperature, pressure, and pressure drop rate) and material compositions on bubble nucleation and growth behaviors.[1–3] These works have identified the optimal processing conditions and material compositions required to produce high quality plastic foams. Moreover, some researchers have designed experimental simulation systems and employed high-speed cameras to capture the *in situ* foaming processes.[4–6] However, because the current experimental techniques cannot probe the process at the molecular level, the bubble nucleation process, which typically happens on the nanometer scale, cannot be explored. As a result, various researchers have resorted to performing theoretical investigations in an attempt to reveal its fundamental mechanisms.[7–11] Most of these studies have been based on the classical nucleation theory,[12,13] which computes the bubble nucleation rate using the following expression:

$$J = J_0 \exp\left(-\frac{W}{k_B T}\right) \tag{1}$$

where J is the number of bubble nucleates per unit volume per unit time; J_0 is the frequency factor; W is the free energy barrier necessary to initiate bubble nucleation; k_B is the Boltzmann constant; and T is the absolute temperature.

For homogeneous nucleation, the free energy barrier, W, can be expressed as:[14]

$$W = W_{hom} = \frac{16\pi\gamma^3}{\left(P_{bubble,0} - P_{sys}\right)^2} \tag{2}$$

where γ is the surface tension of the gas/liquid interface; $P_{bubble,0}$ is the initial pressure inside a critical bubble; and P_{sys} is the system pressure in the polymer–gas solution.

Alternatively, for heterogeneous nucleation, W can be calculated with the following equation:[14]

$$W = W_{het} = \frac{16\pi\gamma^3 F(\theta_c, \beta)}{\left(P_{bubble,0} - P_{sys}\right)^2} \tag{3}$$

where F is a geometrical factor, which is a function of both the contact angle, θ_c, and the semiconical angle, β.[14]

Correspondence to: C. B. Park (park@mie.utoronto.ca).
Contract grant sponsor: Consortium for Cellular and Microcellular Plastics (CCMCP).

Since the cell nucleation process involves clusters consisting of less than one hundred molecules, it is necessary to use a statistical mechanical model to determine $P_{bubble,0}$. However, all of the aforementioned computer simulation studies[7–11] have approximated the values of $P_{bubble,0}$ to be identical to those of the saturation pressure, P_{sat}, when determining W. Although making this substitution helps to simplify the simulation algorithm, the validity of using it in computer simulation has yet to be evaluated.

In this work, the thermodynamic equilibrium condition and the Sanchez–Lacombe (SL) equation of state (EOS) are employed to determine the value of $P_{bubble,0}$. By comparing the computer-simulated cell density using the thermodynamically determined $P_{bubble,0}$, to that according to the approximated $P_{bubble,0}$ with P_{sat}, the impact of using such an approximation on the cell nucleation simulation will be discussed. Although the validity of the SL EOS has not been verified yet,[15] this study will clarify the significance of the error associated with the approximation and provide a way to improve the accuracy of simulating the cell nucleation phenomena in polymeric foaming processes.

Theoretical framework

In the computer simulation of the cell nucleation phenomena, the computation of J in eq. (1) requires an accurate determination of W. By definition, W is the amount of energy possessed by a cluster of gas molecules above which the cluster will grow spontaneously into a larger bubble. In other words, W is the amount of energy required to create a bubble with its radius equal to the critical radius, R_{cr} (i.e., a critical bubble). Therefore, the values of $P_{bubble,0}$ in eqs. (2) and (3) are equal to the gas pressure inside a critical bubble. In nucleation processes, W defines the free energy barrier that the system has to overcome to nucleate a bubble. The process is driven by the degree of supersaturation introduced by decreasing the system pressure and by the thermodynamic fluctuation during the process. Furthermore, nucleation is a kinetic phenomenon. From a theoretical standpoint, it is possible to initiate bubble nucleation by decreasing the system pressure below P_{sat}. However, the bubble nucleation will only be observable if the nucleation rate is sufficiently high. Since nucleation rate increases with the amount of pressure drop, the amount of pressure drop needs to exceed a threshold value to nucleate bubbles in a real process within a finite period of time.

A critical bubble is at an unstable thermodynamic equilibrium state.[14] Thus, the chemical potential of the gas inside the critical bubble, $\mu_{G,bubble}$, and that of the gas in the polymer–gas solution, $\mu_{G,solution}$, can be related by

$$\mu_{G,bubble}(T, P_{bubble,0}) = \mu_{G,solution}(T, P_{sys}, C) \quad (4)$$

where C is the gas concentration in the polymer–gas solution.

During a polymeric foaming process, both P_{sys} and C decrease with time. Since $\mu_{G,solution}$ is known to be a decreasing function of P_{sys} and C, it becomes clear that

$$\mu_{G,solution}(T, P_{sys}, C) \leq \mu_{G,solution}(T, P_{sat}, C_0) \quad (5)$$

where C_0 is the initial concentration of dissolved gas in the polymer–gas solution. The equality in eq. (5) holds only when P_{sys} and C are equal to P_{sat} and C_0, respectively. Furthermore, for a saturated polymer–gas solution with a given gas concentration, C_0, the thermodynamic equilibrium condition can be written as

$$\mu_{G,solution}(T, P_{sat}, C_0) = \mu_{G,bubble}(T, P_{sat}) \quad (6)$$

Therefore, using eqs. (4)–(6), it can be concluded that

$$\mu_{G,bubble}(T, P_{bubble,0}) = \mu_{G,bubble}(T, P_{sat}) \text{ for } t = 0 \quad (7a)$$

$$\mu_{G,bubble}(T, P_{bubble,0}) < \mu_{G,bubble}(T, P_{sat}) \text{ for } t > 0 \quad (7b)$$

where t is the time of the process. Equations 7(a) and 7(b) indicate that the $P_{bubble,0}$ approximation is not valid except at the starting point of the foaming process, although it has been a common practice to approximate it with P_{sat}.[7–11] However, since it is impossible for bubble nucleation to occur when P_{sys} is equal to P_{sat} (i.e., $t = 0$), it is inappropriate to approximate $P_{bubble,0}$ using P_{sat}. Therefore, it is of great interest to evaluate the impact of using this approximation in the computer simulation of the cell nucleation phenomena.

Since the size of a critical bubble is in the submicron level, statistical thermodynamic theories should be employed to determine the chemical potential of the gas in the critical bubble. In this study, following the approach suggested by Li et al.,[16] the values of $\mu_{G,bubble}$ and $\mu_{G,solution}$ at specified values of T, P_{sys}, and C are determined based on the SL EOS, which is expressed as:[17,18]

$$\rho_R^2 + P_R + T_R[\ln(1 - \rho_R) + (1 - 1/r)\rho_R] = 0 \quad (8)$$

where P_R, T_R, and ρ_R are the reduced pressure, temperature, and density of the polymer–gas solution, respectively, and r is the number of lattice sites occupied by a mer.

Using the SL EOS, the values of $\mu_{G,bubble}$ can be determined by eqs. (4) and (8), respectively:[17,18]

$$\mu_{G,bubble} = r_G^0 RT\left[-\frac{\rho_R^G}{T_R^G} + \frac{P_R^G}{\rho_R^G T_R^G} + \left(\frac{1}{\rho_R^G} - 1\right)\ln(1 - \rho_R^G) + \frac{1}{r_G^0}\ln \rho_R^G\right] \quad (9)$$

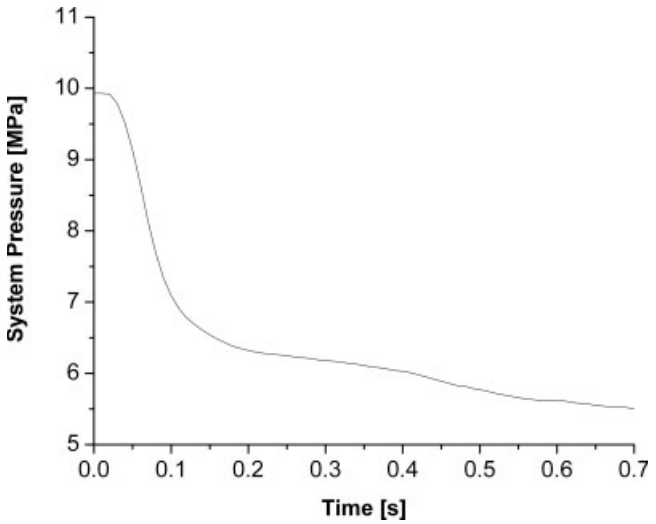

Figure 1 System pressure drop profile of the PS-CO_2 foaming process.

where r_G^0 is the number of lattice sites occupied by a pure gas molecule; R is the universal gas constant; and P_R^G, T_R^G, and ρ_R^G are the reduced pressure, temperature, and density for the gas component, respectively. Similarly, the value of $\mu_{G,solution}$ can be computed by:[17,18]

$$\mu_{G,solution} = RT\left[\ln\varphi_G + \left(1 - \frac{r_G}{r_P}\right)\varphi_P + r_G^0\rho_R X_G{\varphi_P}^2\right] + r_G^0 RT\left[-\frac{\rho_R}{T_R^G} + \frac{P_R^G}{\rho_R T_R^G} + \left(\frac{1}{\rho_R} - 1\right) \times \ln(1-\rho_R) + \frac{1}{r_G^0}\ln\rho_R\right] \quad (10)$$

where φ_G and φ_P are the close-packed volume fractions of the gas and the polymer components; r_G and r_P are the number of lattice sites occupied by a gas molecule and a mer in the polymer–gas mixture; and X_G is a function of the following:

$$X_G = \frac{(P_G^* + P_P^* - 2P_M^*)}{P_G^* T_R^G} \quad (11)$$

where P_G^*, P_P^*, and P_M^* are the characteristic pressures of the gas, polymer, and the polymer–gas mixture, respectively. P_M* can be determined using eq. (12):

$$P_M^* = (P_G^* P_P^*)^{\frac{1}{2}}(1 - K_{12}) \quad (12)$$

where K_{12} is the interaction parameter for the SL EOS.

Consequently, $P_{bubble,0}$ can be estimated by solving eqs. (4) and (9)–(12) simultaneously.

Methodology

This work studies the impact of substituting P_{sat} for $P_{bubble,0}$ in cell nucleation simulations. The study evaluates the cell densities of the computer-simulated polystyrene (PS)-carbon dioxide (CO_2) foaming processes and compares the results with the thermodynamically-determined $P_{bubble,0}$ and those yielded with the $P_{bubble,0}$ approximation. The processing conditions and the material parameters being considered in this work are based on the experimental case studied in our previous work.[14] The system pressure drop profile is illustrated in Figure 1.

The simultaneous simulation of the cell nucleation and growth processes is based on an integrated model that combines the modified nucleation theory[14] and the cell model proposed by Amon et al.[19] Table I summarizes the major differences between this simulation approach and some other methodologies proposed in past researches. For the cell nucleation simulation, the cell density with

TABLE I
Comparison Between Different Foaming Simulation Approaches

	Shaft's approach[9]	Shimoda's approach[11]	Our approach
Determination of $P_{bubble,0}$	Approximated by P_{sat}	Two cases were presented: Case 1, approximated by P_{sat}; Case 2, estimated by the average gas concentration and the Henry's law constant	Determined by the thermodynamic equilibrium condition and SL EOS
Determination of γ_{lg}	Considered the variation of surface tension with cluster size based on the long range intermolecular potential[21]	Approximated by the experimentally measured γ_{lg} without considering the cluster size effect	Considered the variation of surface tension with cluster size based on the Scaling Functional Approach[16]
Determination of C_{avg}	Employed the influence volume approach	Two cases were presented: Case 1 employed the influence volume approach; Case 2 did not consider the influence volume	Did not consider the influence volume
Determination of the concentration profile around each nucleated bubble	Determined by solving the diffusion equation	Approximated by a 4th order polynomial	Determined by solving the diffusion equation

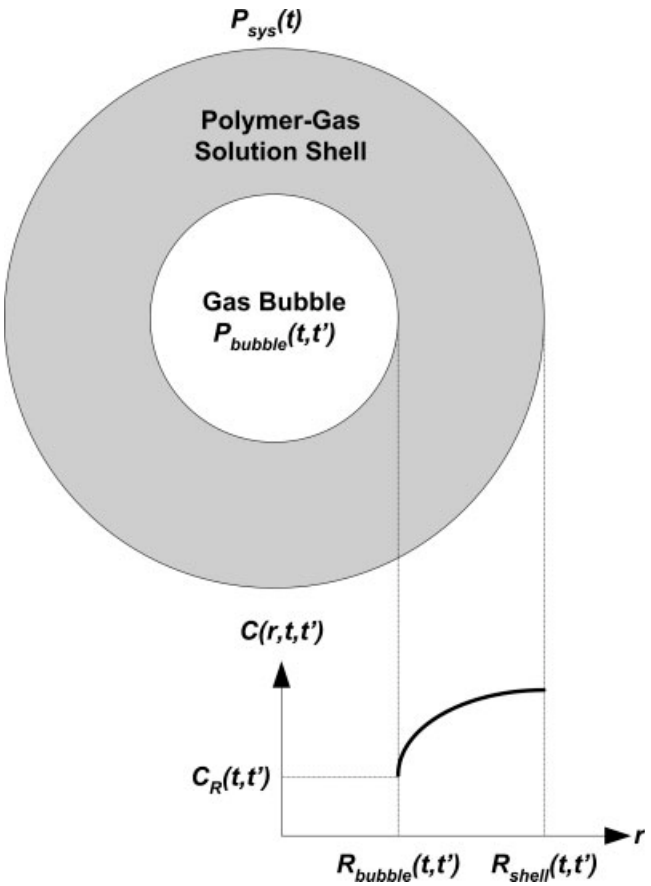

Figure 2 A schematic representation of a gas bubble and its corresponding polymer–gas solution shell.

respect to the unfoamed volume of the polymer at time t, $N_b(t)$, can be computed by

$$N_b(t) = \int_0^t J(t')\, dt' \tag{13}$$

where $J(t')$ is the sum of the homogeneous and heterogeneous nucleation rates, which are determined by eqs. (1)–(3). The value of θ_c is considered to be 86.42°.[14] Moreover, since the heterogeneous nucleation rate is very sensitive to the change of the surface geometry (i.e., β)[20] and the shapes of different nucleating sites are likely to be random, the values of β at different nucleating sites are approximated to follow a normal distribution between 0° and 90°.[14]

The average dissolved gas concentration, $C_{avg}(t)$, that remains in the polymer–gas solution can be determined by

$$C_{avg}(t) = C_0 - \int_0^t \frac{4\pi R_{bubble}(t,t')^3 P_{bubble}(t,t')}{3R_gT}[J(t')]\, dt' \tag{14}$$

where C_0 is the initial dissolved gas concentration; $R_{bubble}(t,t')$ is the bubble radius at time t for the bubble nucleated at time t'; $P_{bubble}(t,t')$ is the bubble pressure at time t for the bubble nucleated at time t'; and R_g is the universal gas constant.

In the case of bubble growth simulation, each bubble is considered to be surrounded by a shell of viscoelastic fluid of finite volume and a limited amount of gas concentration.[22] A schematic representation of a nucleated bubble and its corresponding polymer–gas solution shell is shown in Figure 2. In the figure, $R_{shell}(t,t')$ is the radius of the polymer–gas solution shell for the corresponding bubble; $C(r,t,t')$ is the dissolved gas concentration at radial position r; and $C_R(t,t')$ is the dissolved gas concentration at the bubble surface.

Applying the aforementioned model, the overall simulation algorithm illustrated in Figure 3 is used to calculate the cell density, N_b. The details of this proc-

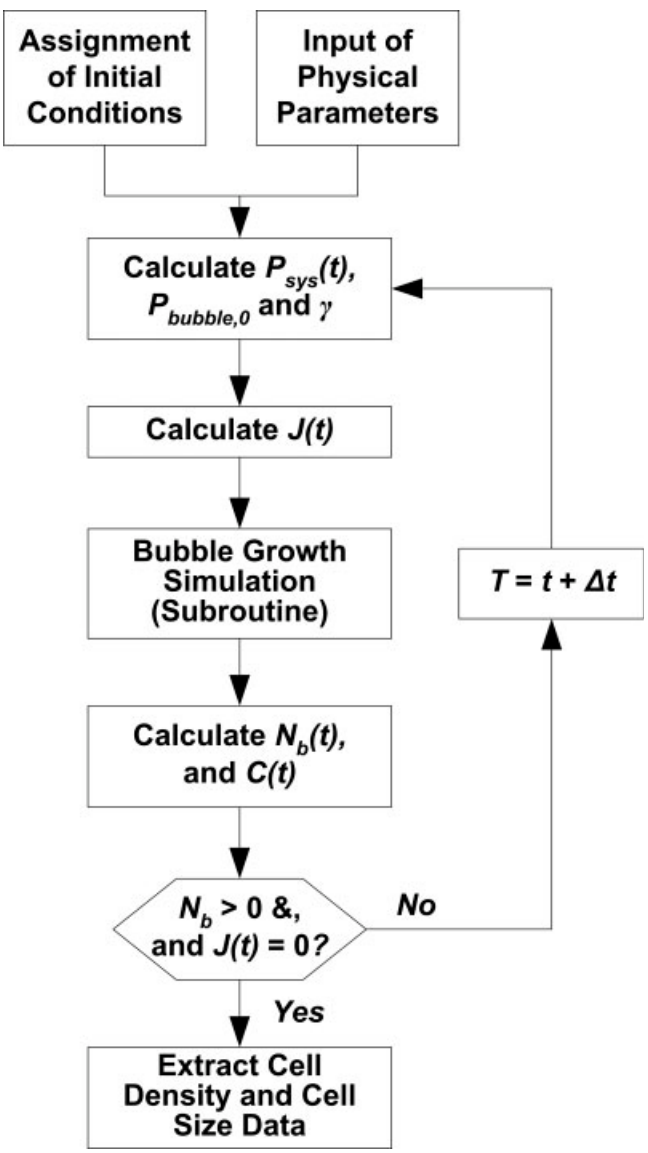

Figure 3 Overall algorithm of the cell nucleation and growth simulations.

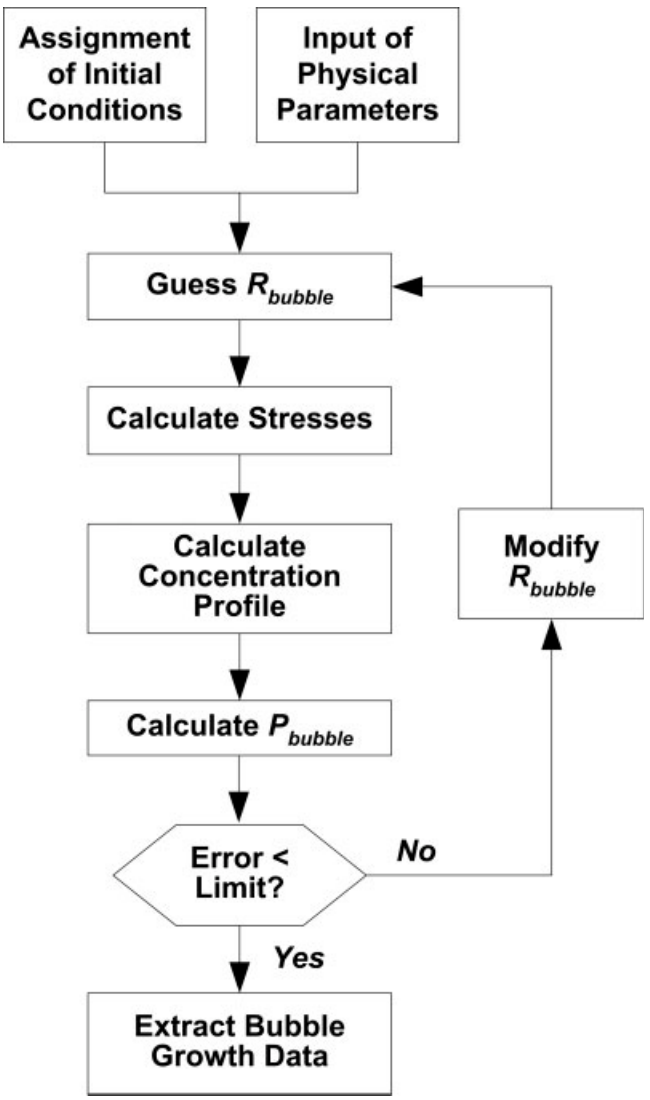

Figure 4 Subroutine for bubble growth simulation.

edure can be found in Ref. 14. The subroutine to compute the bubble growth profiles is shown in Figure 4.

During the simulation, the value of $P_{bubble,0}$ at each time step is required to determine the bubble nucleation rate. To solve for its value using eqs. (4) and (9)–(12), it is necessary to know the values of the characteristic pressures, volumes, and temperatures of PS[15] and CO_2.[23] The values of these parameters are summarized in Table II. Moreover, the value of K_{12} is based on the data obtained by Li et al.[19]

Throughout the course of the simulations, the content of the dissolved gas in the polymer matrix decreases continuously due to the gas consumption by the bubble nucleation and growth processes. Finally, when $C_{avg}(t)$ is sufficiently low, the nucleation rate is negligible and this point is considered to be the termination point of the simulation. Consequently, information about the cell density and the bubble radii for each time step was extracted from the simulation program for the subsequent analyses.

TABLE II
Characteristic Parameters for the SL EOS

Substance	P^* (MPa)	V^* (cm^3/g)	T^* (K)
PS	410.35	0.9093	746.1
CO_2	720.30	0.6329	$208.9 + 0.459\ T - 7.56 \times 10^{-4}\ T^2$

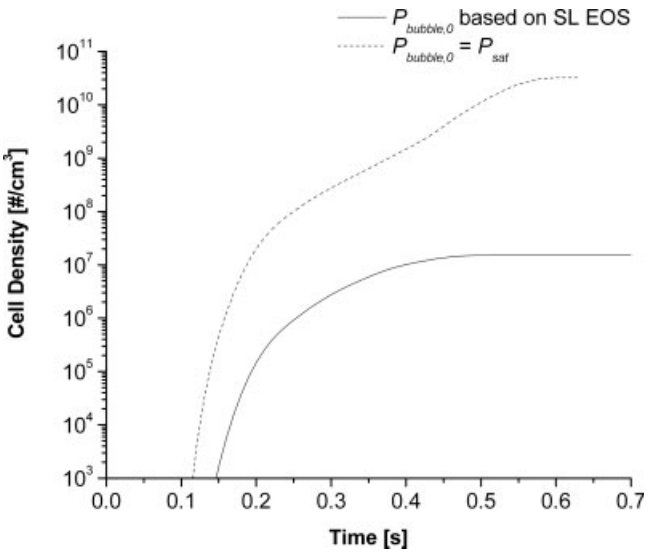

Figure 5 Effect of the $P_{bubble,0}$ approximation on the predicted cell density.

RESULTS AND DISCUSSION

Following the aforementioned approach, numerical simulation was performed to study the effect of $P_{bubble,0}$

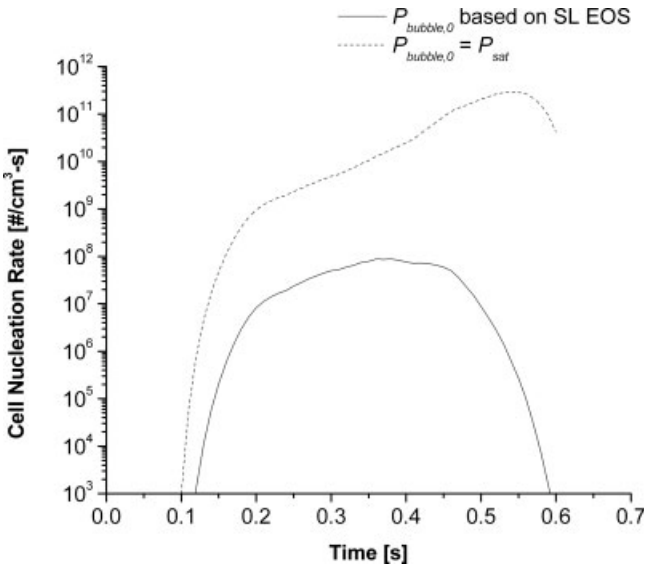

Figure 6 Effect of the $P_{bubble,0}$ approximation on the predicted cell nucleation rate.

approximation on the cell nucleation phenomena in the polymeric foaming process. Figure 5 demonstrates that the $P_{bubble,0}$ approximation will lead to a significant overestimation — by as much as three orders of magnitude — of the final cell density. Furthermore, the results show that such an approximation will result in an earlier onset time of the bubble nucleation process. These results are due to the higher cell nucleation rate when P_{sat} is employed to approximate $P_{bubble,0}$ as illustrated in Figure 6.

Figure 6 indicates that the highest nucleation rate computed using the $P_{bubble,0}$ approximation is about 10^{11} bubbles/cm^3/s, which is about three orders of magnitude higher than that calculated using the thermodynamically determined $P_{bubble,0}$. Furthermore, because of the elevated nucleation rate, the predicted gas consumption rate was higher as suggested in Figure 7. Consequently, the average gas content will decrease more rapidly if the approximation is adopted.

To elucidate the effects of the $P_{bubble,0}$ approximation on predicting the cell density, the cell nucleation rate, and the average gas content, it would be interesting to analyze the deviation of $P_{bubble,0}$ from P_{sat} during the polymeric foaming process. Figure 8 shows that $P_{bubble,0}$ and P_{sat} are equal only when P_{sys} is the same as P_{sat}. When P_{sys} was decreasing rapidly during the foaming process, $P_{bubble,0}$ also decreased continuously and deviated from P_{sat}. Moreover, it can be observed that $P_{bubble,0}$ started to decrease more rapidly after $\sim$ 0.4 s because of the significant depletion of the dissolved gas content (see Fig. 7).

The driving force of cell nucleation can be expressed as

$$\Delta P = P_{bubble,0} - P_{sys} \quad (15)$$

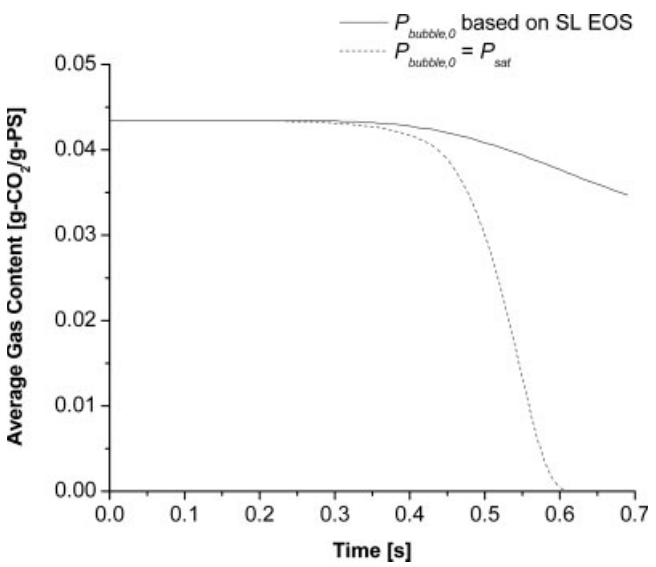

Figure 7 Effect of the $P_{bubble,0}$ approximation on the predicted average gas concentration in the PS-CO_2 solution.

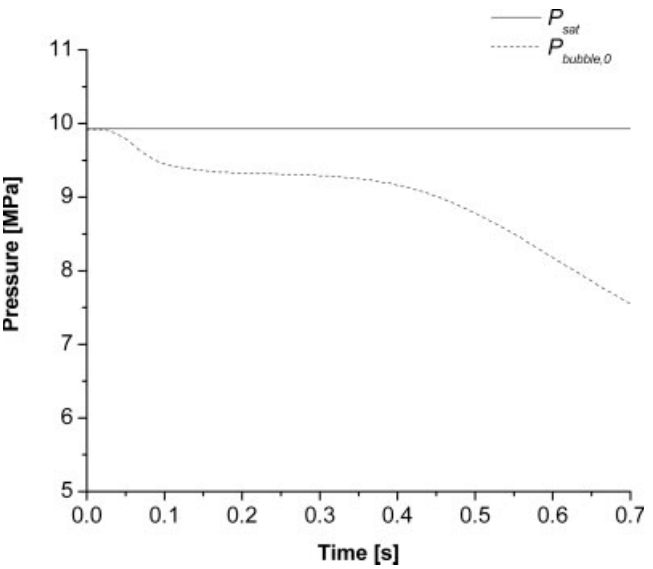

Figure 8 Deviation of $P_{bubble,0}$ from P_{sat}.

Therefore, the results illustrated in Figure 8 indicate that the approximation of $P_{bubble,0}$ using P_{sat} significantly exaggerates the magnitude of ΔP, especially in the later stages of the foaming process. Using eqs. (1)–(3), it can be concluded that the $P_{bubble,0}$ approximation significantly underestimates the free energy barrier for bubble nucleation and thereby leads to overestimations regarding the cell density, the cell nucleation rate, and the dissolved gas consumption rate.

CONCLUSION

This study analyses the impact of approximating the initial bubble pressure (i.e., $P_{bubble,0} = P_{sat}$) in the simulation of the nucleation phenomena in the polymeric foaming processes. It was observed that the simulation result using the approximation predicts an earlier onset time for bubble nucleation. Moreover, it also significantly overestimates the final cell density, the bubble nucleation rate, and the dissolved gas consumption rate. Therefore, the approximation should be avoided in the numerical simulation of the foaming processes.

References

1. Park, C. B.; Baldwin, D. G.; Suh, N. P. Polym Eng Sci 1995, 432, 35.
2. Naguib, H. E.; Park, C. B.; Lee, P. C. J Cell Plast 2003, 499, 39.
3. Lee, J. W. S.; Wang, K. H.; Park C. B. Ind Eng Chem Res 2005, 1, 44.
4. Ohyabu, H.; Otake, K.; Hayashi, H.; Inomama, H.; Taira, T. PPS19, Australia 2003.
5. Taki, K.; Nakayama, T.; Yatsuzuka, T.; Ohshima, M. J Cell Plast 2001, 517, 37.
6. Guo, Q.; Wang, J.; Park, C. B.; Ohshima, M. SPE ANTEC Tech Papers, No. 510, May 16–19, 2004.

7. Han, J. H.; Han, C. D. J Polym Sci 1990, 28, 743.
8. Lee, J. G.; Flumerfelt, R. W. J Colloid Interface Sci 1996, 184, 335.
9. Shafi, M. A.; Joshi, K.; Flumerfelt, R. W. Chem Eng Sci 1997, 52, 635.
10. Joshi, K.; Lee, J. G.; Shafi, M.; Flumerfelt, R. W. J Appl Polym Sci 1998, 67, 1353.
11. Shimoda, M.; Tsujimura, I.; Tanigaki, M.; Ohshima, M. J Cell Plast 2001, 37, 517.
12. Gibbs, J. W. The Scientific Papers of J Willard Gibbs, Vol. 1; Dover: New York, 1961; p. 337.
13. Blander, M.; Katz, J. L. ALChE J 1975, 21, 833.
14. Leung, S. N.; Park, C. B.; Li, H. Plast Rubber Compos 2006, 35, 93.
15. Li, G.; Wang, J.; Park, C. B.; Moulinie, P.; Simha, R. SPE ANTEC Tech Papers, No. 421, May 16–19, 2004.
16. Li, H.; Leung, S. N.; Park, C. B; Li, G. SPE ANTEC Tech Papers, No. 101327, May 1–4, 2005.
17. Sanchez, I. C.; Lacombe, R. H. Macromolecules 1976, 80, 2352.
18. Sanchez, I. C.; Lacombe, R. H. Macromolecules 1978, 11, 1145.
19. Amon, M.; Denson, C. D. Polym Eng Sci 1984, 26, 1026.
20. Xu, D.; Li, H.; Fenton, R. G. Ind Eng Chem Res 2006, 45, 7823.
21. Lee, J. G.; Flumerfelt, R. W. J Colloid Interface Sci 1996, 184, 335.
22. Leung, S. N.; Park, C. B.; Xu, D.; Li, H.; Fenton, R. G. Ind Eng Chem Res, in press.
23. Sato, Y.; Yurugi, M.; Fujiwara, K.; Takishima, S.; Masuoka, H. Fluid Phase Equilibria 2001, 125, 187.